Silicon/Zinc Sulfide Multi-Quantum-Well Structures for Inter-subband Lasers

GRANT NUMBER: F49620-96-1-0242
START DATE: JUNE 1, 1996

Final Report

DECEMBER 31, 1999

PRINCIPAL INVESTIGATOR:

Wiley P. Kirk

Center for Nanostructure Materials & Quantum Device Fabrication
Engineering-Physics Building
Texas A&M University System
College Station, Texas 77843-4242
PH: 409-845-1179
FAX: 409-845-2590
kirk@nanofab.tamu.edu

REPORT DOCUMENTATION PAGE

AFRL-SR-BL-TR-00-

0798

1. AGENCY USE ONLY *(Leave blank)*	2. REPORT DATE	3. RL
		01 Jun 96 to 30 Ap 99 Final

4. TITLE AND SUBTITLE
Silicon/Zinc Sulfide multi-Quantum-Well structures for intersub-band lasers

5. FUNDING NUMBERS
61102F
2305/FS

6. AUTHOR(S)
Professor Kirk

7. PERFORMING ORGANIZATION NAME(S) AND ADDRESS(ES)
Texas Engineering Experiment Station
332 Wisenbaker Eng Res Center
College Station TX 77843-3000

8. PERFORMING ORGANIZATION REPORT NUMBER

9. SPONSORING/MONITORING AGENCY NAME(S) AND ADDRESS(ES)
AFOSR/NE
801 North Randolph Street Rm 732
Arlington, VA 22203-1977

10. SPONSORING/MONITORING AGENCY REPORT NUMBER
F49620-96-1-0242

11. SUPPLEMENTARY NOTES

12a. DISTRIBUTION AVAILABILITY STATEMENT
APPROVAL FOR PUBLIC RELEASED; DISTRIBUTION UNLIMITED

12b. DISTRIBUTION CODE

13. ABSTRACT *(Maximum 200 words)*

Reduced cross-contamination, development of a new process to improve thin-layer growth, more precise control of the thicknesses of both Si and ZnS epitaxial layers, reduced fixed charge density in the ZnS or at the ZnS/Si interface, reduced mobile charge in the ZnS, determination of the band offset between ZnS and Si to be 1.0 ± 0.1 eV and development of a new class of wide bandgap Be-chalcogenide materials.

14. SUBJECT TERMS

15. NUMBER OF PAGES

16. PRICE CODE

17. SECURITY CLASSIFICATION OF REPORT	18. SECURITY CLASSIFICATION OF THIS PAGE	19. SECURITY CLASSIFICATION OF ABSTRACT	20. LIMITATION OF ABSTRACT
UNCLASSIFIED	UNCLASSIFIED	UNCLASSIFIED	UL

Objectives

The goal of this project was to develop a suitable silicon-based heterostructure material system (or systems) for use as inter-subband low-threshold semiconductor lasers. These devices would serve as optical link structures for optoelectronic information processing applications. To achieve this goal the program was divided into four tasks:

Task 1 Develop Single and Multi-Quantum Well Structures for Optical Absorption Measurements, Waveguide Studies, and Low-Threshold Inter-subband Laser Devices.

This task entailed depositing by molecular beam epitaxy and delivering to Hanscom AFB single and multi-quantum well Si/ZnS structures for optical absorption studies. The theoretical modeling results from the Hanscom AFB group, as well as the optical absorption data, would be used to optimize growth parameters. Undertake the construction of a new type of optical waveguide structure using silicon-on-insulator (SOI) substrates. Also explore the possibility of developing a photosensitive PIN diode structure.

Task 2 Refine Doping Techniques, Measure Current Leakage and Threshold Effects

This task was to test the idea of using boron doping to shift the Si quantum wells from weak n-type to strong p-type doping. This required the design and construction of apparatus to separate growth and passivation deposition steps in order to eliminate uncontrolled doping from background constituents. Conduct current-voltage measurements and investigate current leakage and threshold effects in suitably doped structures.

Task 3 Evaluate Interface Quality

This task required the determination of the quality of the heterostructure interfaces by measuring the density of interface states using capacitance-voltage (C-V) techniques. Examine the interface quality on the atomic scale using cross-section transmission electron microscopy procedures and cleaved-edge scanning tunneling microscopy techniques.

Task 4 Determine Band Offsets

This task involved the measurement of valence band offsets by a several methods including C-V, Kelvin probe, ultraviolet photoresponse, and cross-section scanning tunneling microscopy.

Summary of Effort

A large number of ZnS films were grown epitaxially on Si using a monolayer of As to passivate and control the interface between the polar and nonpolar species. Additional structures were grown with Si deposited epitaxially on the ZnS to form Si/ZnS/Si-substrate single-barrier structures. A double-barrier structure with Si quantum well was grown and delivered to Rome Laboratory for photo-luminescence evaluations. It was then determined that the single-growth-chamber apparatus used in these studies limited our ability to control growth processes well enough to form reliable thin epitaxial layers needed for quantum well formation. To overcome these limitations a new growth chamber was installed and additional modifications were made to the existing apparatus. These modifications led to significant improvements and opened the door for the exploration of an entire new set of candidate materials to develop Si-based heterostructures for laser and optical waveguide applications. The main results of the project, resulting from growth, measurement, and new apparatus modifications, include the following:

- Reduced cross-contamination.
- Development of a new process to improve thin-layer growth.
- More precise control of the thicknesses of both Si and ZnS epitaxial layers.

- Reduced fixed charge density in the ZnS or at the ZnS/Si interface.
- Reduced mobile charge in the ZnS.
- Determination of the band offset between ZnS and Si to be 1.0 ± 0.1 eV.
- Development of a new class of wide bandgap Be-chalcogenide materials.

The experimental results indicated that ZnS can be used to form the barriers for Si quantum wells, but the growth conditions must be controlled very carefully. New preliminary studies presented in this report indicate that the beryllium-chalcogenides may be more robust and a more easily managed wide bandgap system for inter-subband laser applications.

Task 1

Progress on this task was made when we found and used an As passivation method to successfully grow epitaxial ZnS layers on Si substrates. By comparison, we achieved successful but inconsistent results when we tried growing Si layers on ZnS. Both ZnS/Si single barrier and Si/ZnS/Si double barrier (single quantum well) structures were grown by molecular beam epitaxy (MBE), but the wells and barriers were not as thin as desired. In any case, a quantum well structure was delivered to Dr. Soref at Hanscom AFB for photoluminescence studies. A strong PL line at 1.3 eV (950.6 nm) was observed and thought to possibly arise from the silicon quantum well. We were not able to confirm this result because of difficulties in growing reliable quantum-well structures. In order to achieve thinner layers and more reproducible Si regrowth on ZnS, we reached the conclusion that the apparatus needed to be modified considerably to eliminate cross-contamination effects caused by use of too many material groups in the same growth chamber.

Task 2

Progress on this task was made through the installation of a new II-VI growth chamber to separate growth of Si, As, and ZnS. This new installation allowed us to separate the growth, doping, and passivation steps. In addition high frequency C-V measurements and I-V measurements were made. From the I-V measurements we found that the leakage current was only about 10^{-10} (A/cm^2) even at 1.0 V and that the breakdown field in the ZnS was over 1 MV/cm.

Task 3

The interface quality was studied by way of electrical measurements, cross-section transmission electron microscopy (TEM), and cleaved-edge scanning tunneling microscopy (STM) studies on samples sent to Professor Joseph Lyding's group at the University of Illinois.

Task 4

With respect to this task, accurate band offset results were obtained and cross-checked by two measurement techniques. The first technique involved a thermionic emission method in which the I-V current was measured at different temperatures. This technique yielded a value of 1.1 ± 0.1 eV for the conduction band-offset between ZnS and Si. A second technique involved formation of a Si/ZnS/Si single tunneling barrier and measurement of the I-V curve. The technique yielded a room temperature value of 1.0 eV for the conduction band-offset. Because the two measurements were done separately, we believe that the value 1.0 ± 0.1 eV for the conduction band-offset is reliable. From the standpoint of considering only the band structure, it is clear that a ZnS/Si quantum well structure is a suitable candidate for an inter-subband laser application.

The results of Task 4 were transferred to Dr. Soref at Hanscom AFB for theoretical modeling purposes. The modeling effort lead to two publications. [L. C. Lew Yan Voon, L. R.

Ram-Mohan and R. A. Soref, *Electronic and optical properties of (001) Si/ZnS heterostructures*, Applied Physics Letters 70, 1837-1839 (7 April 1997). R. A. Soref, L. Friedman, L. C. Lew Yan Voon, L. R. Ram-Mohan, and G. Sun, *Progress toward silicon-based intersubband lasers*, oral presentation (and manuscript) at Silicon Heterostructures Conference, Barga, Italy, 15 Sept 1997.]

Accomplishments and New Findings

1. Single quantum-well growth and photoluminescence studies

In Figure 1, we show a TEM cross-section micrograph of a double-barrier structure (a-Si/ZnS/Si/ZnS/Si substrate) we grew under the constraints imposed by a single growth chamber apparatus we used initially in the project. Although the quality of these structures was not high, we improved the structures considerably with apparatus modifications described later in this report. Nevertheless samples of this type were sent to Dr. Soref at Hanscom AFB for photoluminescence studies. In Figure 2 we show high sensitivity photoluminescence spectra produced by these quantum well structures (with the top contact-layer removed). Measurements were done at liquid helium temperature, 4K, using lock-in detection and excitation by a 488 nm argon ion laser. The well-known PL lines from the silicon substrate were observed, as well as some new features: strong PL line at 1.30 eV (951 nm), medium PL line at 1.37 eV (898 nm), medium PL line at 1.41 eV (876 nm). The interpretation of these lines remain open to question. It is difficult to say without a doubt that this infrared emission came from the silicon quantum well. It may indeed have come from the QW, but this needs to be demonstrated more convincingly.

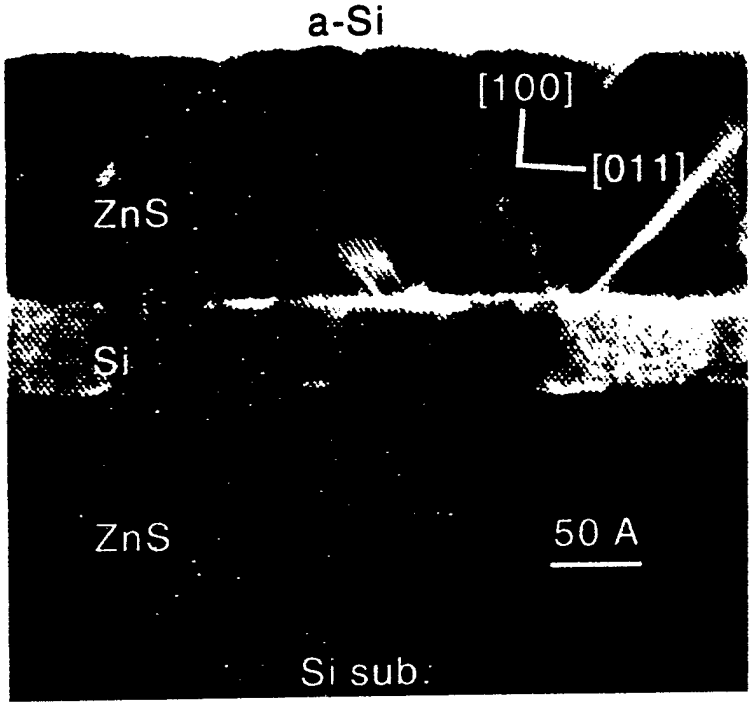

Figure 1 Bright-view, cross-sectional TEM micrographs of a double barrier structure a-Si//ZnS/Si/ZnS/As/Si(100). The structure was capped with amorphous silicon of 300 Å thickness, which shows low contrast in this digitized image. A vicinal Si(100) substrate with a 4° offcut towards [011] direction was used.

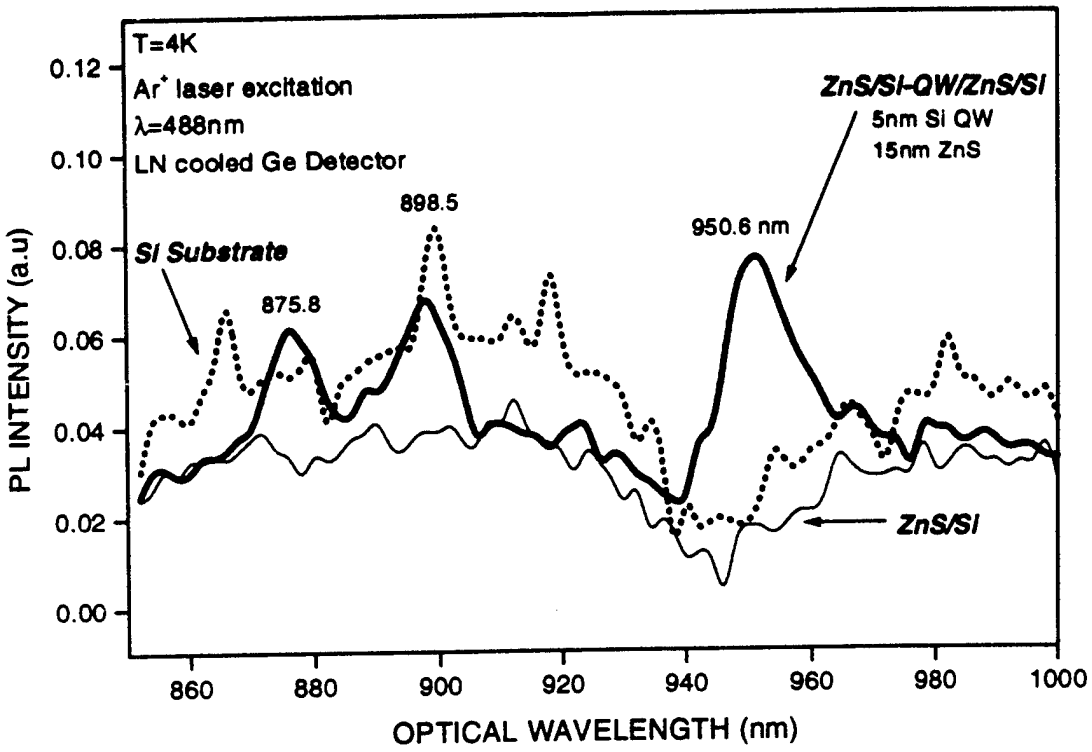

Figure 2 Photoluminescence spectra a Si/ZnS/Si/ZnS/Si quantum well measured at USAF Rome Laboratory by Dr. Darlene Schwall.

2. Interface quality and assessment of thermal stability limits of ZnS

In order to produce effective barrier structures of ZnS on Si for optoelectronic devices, it was necessary to establish methods of growing ZnS layers thinner than 40 Å (about 15 monolayers). Therefore, growing thin ZnS layers and carefully controlling the thickness of the layers represented an important step in the overall goal of the project. In Figure 3 we show the ability to successfully grow several thin single-barrier ZnS structures. The layer thickness of these structures was measured by cross-sectional transmission electron microscopy (TEM), over a range of 7 (19.0 Å), 8 (21.7 Å), 13 (35.2 Å), and 18 (48.7 Å) monolayers (Ångströms), respectively. Samples similar to these, but with slightly thicker layers, were sent to Professor Lyding's group at the University of Illinois for cross-sectional analysis using cleaved-edge scanning probe microscopy.

3. Determination of the band offset for a ZnS/Si heterojunction

One accomplishment achieved as part of this project was the determination of the band offset for the ZnS/Si heterojunction. From this result one can proceed to exploit more effectively this wide-bandgap/narrow-bandgap system for AFOSR's initiative to develop low-threshold semiconductor lasers for efficient free-space interconnects. This result addressed **Task 4**, done partially under this grant.

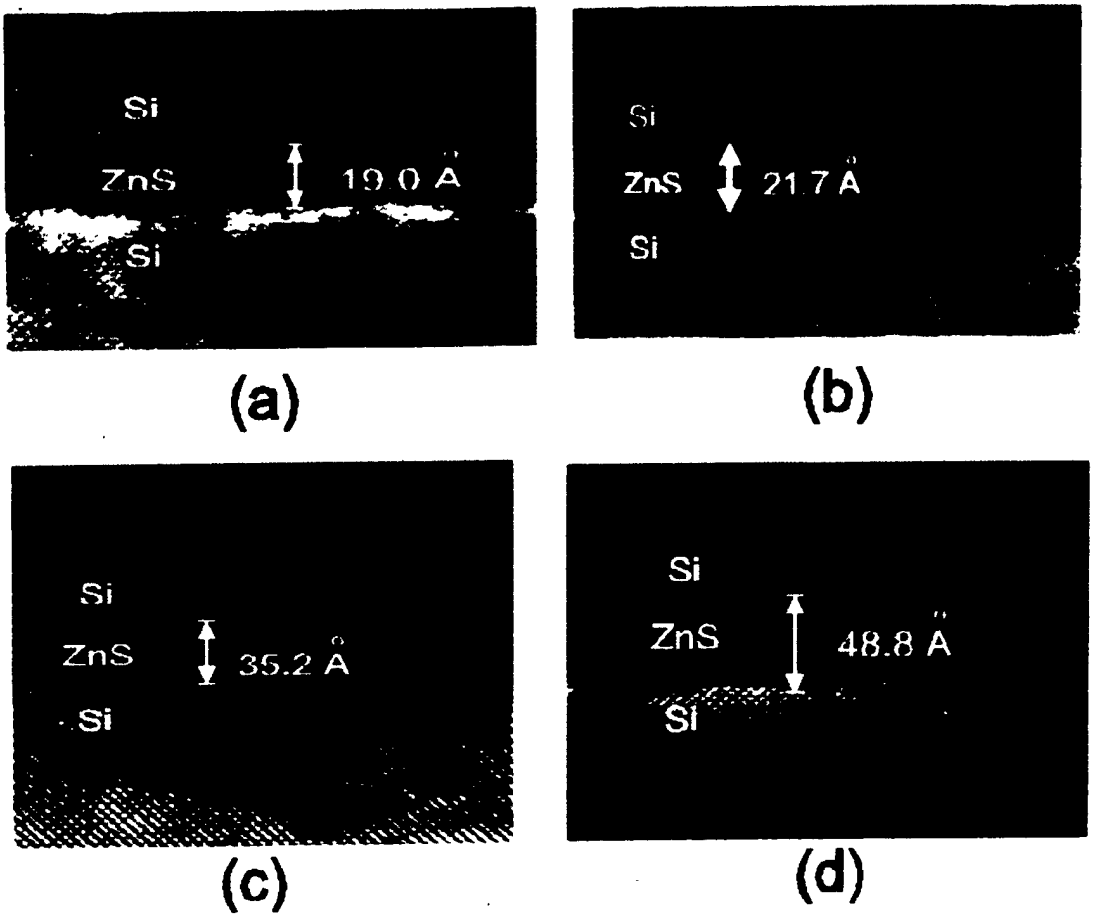

Figure 3 TEM images of four Si/ZnS/Si single-barrier structures.

Two types of single-barrier silicon-based heterojunctions [ZnS/Si(100) and Si/ZnS/Si(100)] were grown by MBE and two types of measurements were made to obtain a conduction band offset value for a ZnS/Si heterojunction. For the first, Type I, measurement a MIS [Al/ZnS/Si] structure was formed and the thermionic emission current was measured. Some of the MIS structures were fabricated by NanoFAB Center personnel, while others were made by Texas Instruments personnel. The bias voltage was scanned from 0 - 2.0 V and the device temperature was changed from 270 K to 470 K. Representative experimental results are shown in Figure 4. Since the ZnS layer in the MIS structure was very thick, about 2000 Å, the thermionic emission current dominated conduction and was expected to be exponentially dependent on temperature. The thermionic measurements were performed in the Texas Instruments laboratories by Mr. Robert Steinhoff, a MIT student on an industrial study assignment, and by Dr. Bobby Brar a member of the technical staff at Texas Instruments.

A semilogarithmic plot of J_0 / T^2 (where J_0 is the current density) versus inverse temperature T is shown in Figure 5. From Figure 5 it is clear that when the temperature is higher than 373 K, $\log(J_0 / T^2)$ displays a linear dependence with inverse temperature.

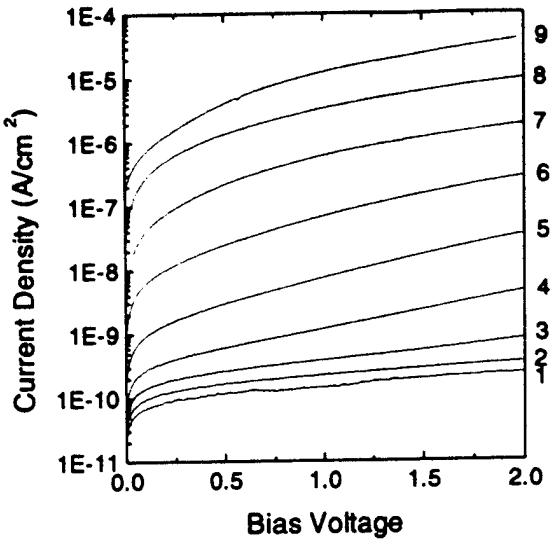

Figure 4 I-V characteristics of ZnS/Si MIS structure at different temperatures. Curves 1, 2, 3, 4, 5, 6, 7, 8, and 9 correspond to temperatures 270 K, 295 K, 320 K, 345 K, 370 K, 395 K, 420 K, 445 K, and 470 K, respectively.

Because of band bending effects due to applied bias potentials, the slopes of the curves in Figure 5, which were related to the conduction band offset, were voltage dependent. The true conduction band offset at zero bias potential was therefore obtained from the re-plotted data shown

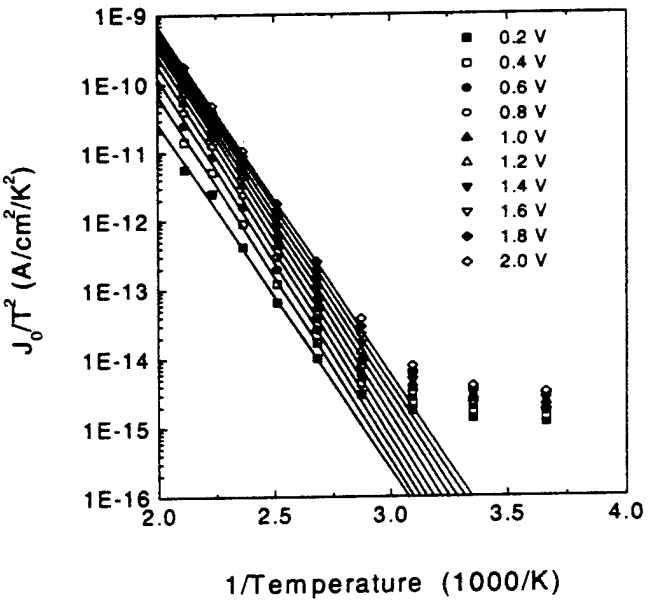

Figure 5 Semilogarithmic plot of current density divided by temperature squared versus inverse temperature for ZnS/Si MIS structure as a function of different bias voltages.

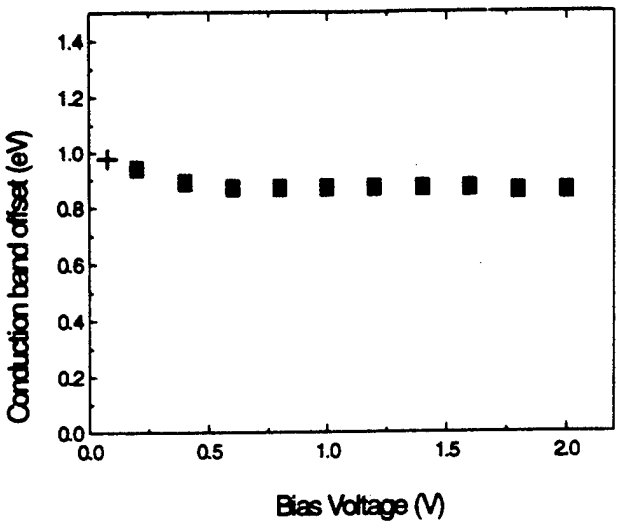

Figure 6 Conduction band offset between ZnS and Si as measured at different bias voltages. Data shown by "■" were the thermionic emission results and "+" was the single-barrier tunneling result.

in Figure 6. Using this procedure we determined that the conduction band offset for ZnS/Si was 1.1±0.1 eV as measured by the thermionic emission technique.

The second, Type II, method we used to determine the conduction band offset was done by using molecular beam epitaxy (MBE) to fabricate a thin single-barrier structure, Si(1000 Å)/ ZnS(21.7 Å)/Si(substrate) as shown in Figure 7. Next we deposited metal contacts and measured the I-V characteristics of the barrier tunneling current as a function of temperature. Measurements

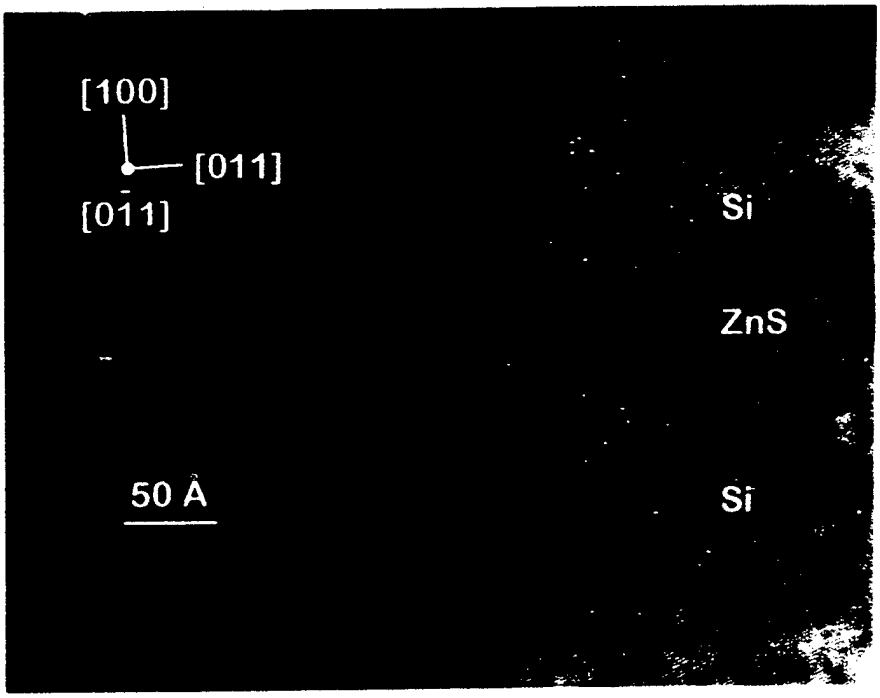

Figure 7 Cross-sectional TEM image of a Si/ZnS/Si(100) structure.

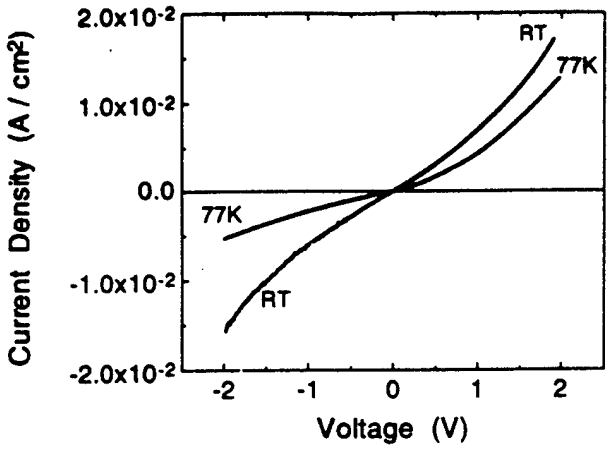

Figure 8 I-V curves of a single barrier structure, shown in Figure 7, measured at room temperature and at 77K.

at two typical temperatures are shown in Figure 8. The experimental I-V characteristic was then compared with a simulated I-V curve produced by the NEMO code developed at Texas Instruments under the guidance of Dr. Roger Lake. The calculation procedure was based on first principles and required only the effective mass and the barrier thickness as input parameters. By using known values for the various semiconductor parameters needed by the code it was possible to extract an offset value of 1.0 ± 0.2 eV. This comparison is shown in Figure 9.

In Figure 6 we show the offset value determined by the Type II method as a single point +. It is clear that the band offsets obtained by the two methods (single-barrier tunneling and thermionic emission) are in good agreement. Because the two measurements were done separately, we believe

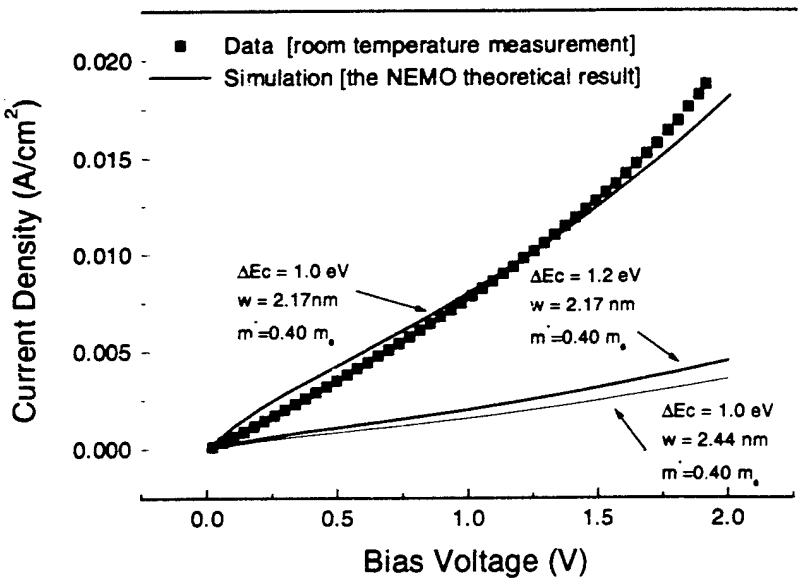

Figure 9 Comparison of experimental and simulated tunneling currents versus bias voltage for a Si/ZnS(21.7 Å)/Si single-barrier structure.

that the value 1.1±0.1 eV for the conduction band offset of ZnS/Si is a reliable result. This result is especially important for future theoretical modeling of electronic and optical behavior based on Si-based heterostructures of these types of materials. A paper reporting these results was prepared for publication.

4. Development of a technique to produce a quantum-well between ZnS and SiO_2 barriers

One of the tasks of this program was to produce waveguide structures with high barriers and silicon quantum wells. However, in principle, there is no reason to require the barriers be constructed of the same material. Some of our initial plans called for the use of SOI substrates to develop waveguide structures. In earlier work, the NanoFAB Center demonstrated success in fabricating single-barrier structures of ZnS with high quality single crystal Si regrown on top of the barrier. Using this structure as the starting point, an opportunity presented itself to build a second barrier of SiO_2 on top by relatively simple means. For example, an ultraviolet/ozone (UV/O_3) method can be used to grow an ultrathin, self-limiting layer of SiO_2 in a single crystal Si regrowth layer. Many groups have demonstrated this UV/O_3 technique.

The NanoFAB Center pursued this procedure by installing a UV/O_3 system into a Reinberg-style plasma etcher The process proceeded by flowing O_2 into the chamber and illuminating it with deep-ultra-violet (DUV) light at 185 nm. This produced ozone, which promoted oxide growth at ambient temperature. The assembled system is shown schematically in Figure 10. One expected advantage of this design was that it is possible to conveniently grow single-barrier layers, Si/ZnS/Si, in our MBE system with a reasonable thickness of regrown Si on the top, say on the order of

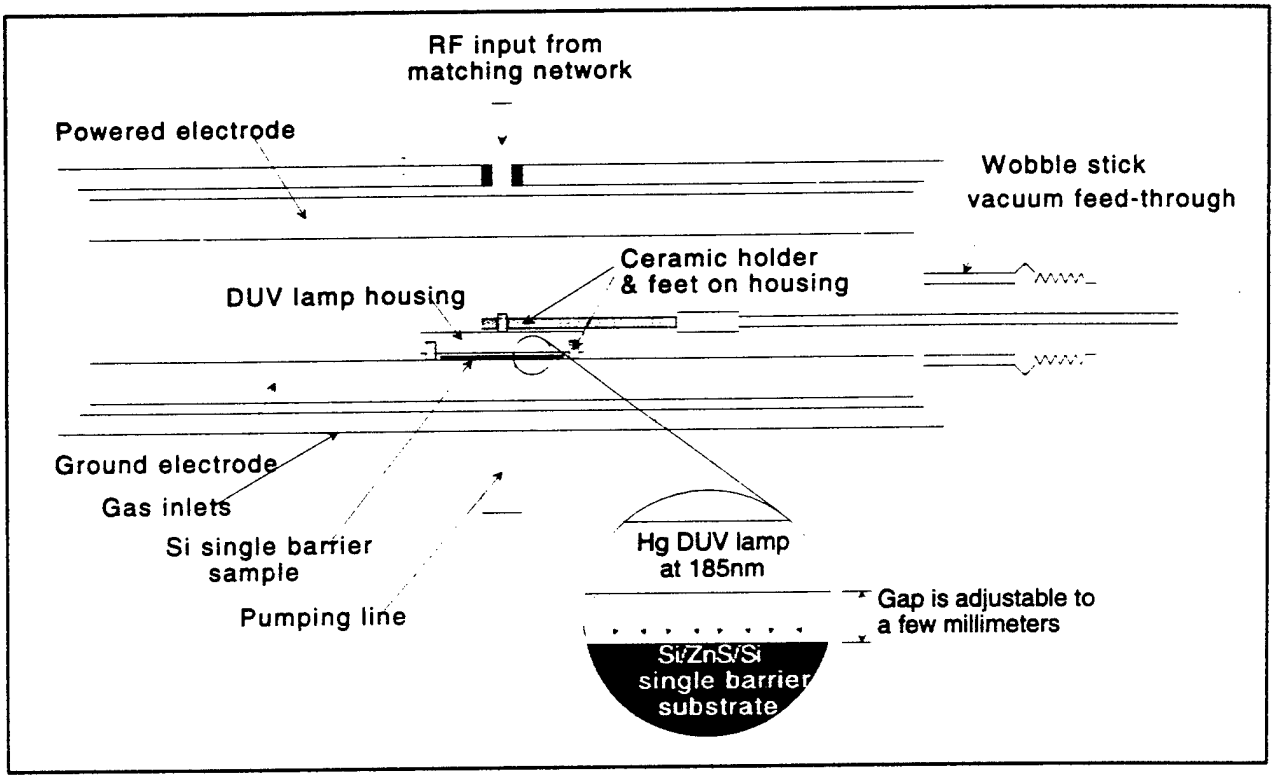

Figure 10 Schematic cross-section of the UV/O_3 lamp mounted inside a plasma etcher. In this configuration, the sample was mounted on the ground electrode. It can be mounted on the upper powered electrode if needed for processing purposes.

100's-to-1000's of Ångströms. Any required surface preparation could then be performed to address flatness or cleanliness issues. Next the upper Si layer could be thinned inside the plasma etcher to the necessary thickness to provide just enough silicon for both the quantum well and for the oxide barrier, both thicknesses ~10-20 Å. The available thinning methods include low-energy ion-milling with Ar or plasma etching with SF_6, which in our reactor could be a very gentle process. The DUV lamp was mounted on a wobble stick to move it aside for plasma processing. Once the thinning process was completed, the lamp could be placed over the sample, O_2 was backfilled into the chamber (or flow may be used), and DUV exposure was begun to form the thin SiO_2 barrier. After considerable experimentation, we abandoned this technique because we could not control layer thickness accurately enough. A different technique was eventually made to work, but that work was done under another project and reported elsewhere.

5. Installation of new growth apparatus to improve quality of heterostructures

After studying various ZnS/Si structures such as MIS structures consisting of thick layers of ZnS grown on Si and single-barrier structures involving thin layers of ZnS sandwiched between Si layers, we attempted to grow double-barrier ZnS/Si heterostructures. We discovered that the quality of these layers was limited significantly by cross contamination between ZnS, Si, and As sources which were used in a single growth chamber. This created a cross-contamination problem that had to be addressed in order to achieve high-quality devices.

One of the existing growth chambers shown schematically in Figure 11, labeled VG V80S, was designed for the growth of group IV materials and was equipped with two e-beam sources for Si and Ge as well as two effusion cells for n- and p-type dopants. We had been using this system to grow II-VI materials such as ZnS epilayers and ZnS/Si single-barrier and double-barrier heterostructures. Growth of these structures required As passivation at the ZnS/Si interface to

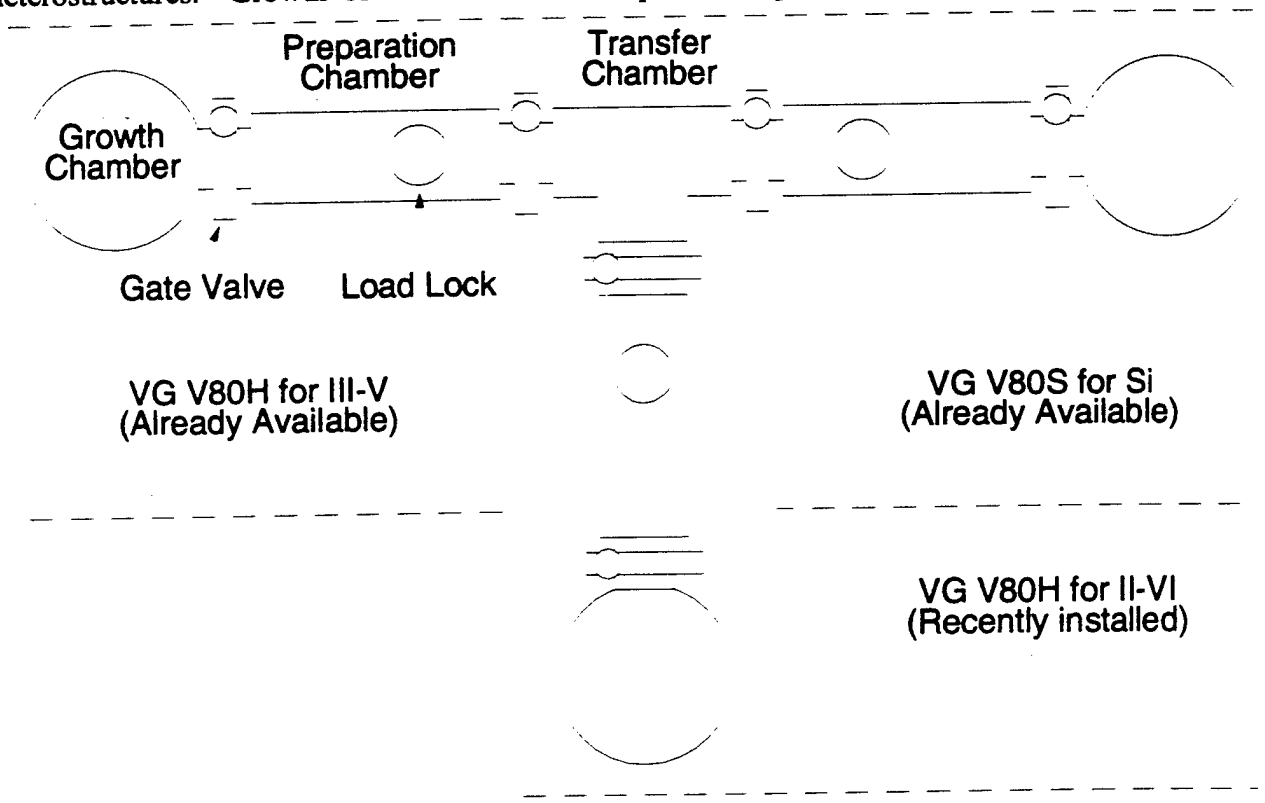

Figure 11 Top-view layout of the multi-chamber heterostructure growth system.

Figure 12 New II-VI growth chamber shown in the center was attached via the transfer chamber to the Si growth system on the right. The III-V growth system, in the background on the right, is barely visible from this view.

eliminate the chemical interaction of S with Si surface. Having all these source materials, *viz.* Si, ZnS, and As, in the same growth chamber resulted in cross contamination of the sources and cell shutters as well as the chamber itself. The other existing growth chamber, labeled VG V80H for III-V, contained effusion cells such as Ga, Al, As, Si, and Be. This chamber was used for the growth of III-V materials such as GaAs and AlGaAs.

To overcome these limitations we purchased a new growth chamber, labeled VG V80H for II-VI in Figure 11, and a transfer chamber. Funding for this purchase came in part from a DURIP equipment grant (DAAHO4-96-1-0363) and partly from this grant. The new growth chamber pictured in Figure 12 was used to grow II-VI materials such as ZnS. The existing VG V80S and VG V80H growth chambers and the new VG V80H growth chamber were linked together by the transfer chamber. We were then able to grow ZnS/Si heterostructures by simply transferring the substrate between these three growth chambers under ultra high vacuum. Each individual chamber is separated from the transfer chamber by a gate valve. This design minimized cross contamination and maintained independent operation of a multi-chamber MBE system.

6. Interface Quality and Cross-Contamination Improvements

(a) Reduced cross contamination

As mentioned, during an early stage of this project, we only had available one growth chamber. With this arrangement, we grew samples using group II, IV, V, and VI elements in the same chamber. Although mixing these groups was clearly not advisable, we nevertheless were able to demonstrate that epitaxial quality ZnS layers could be grown on Si. However, the cross

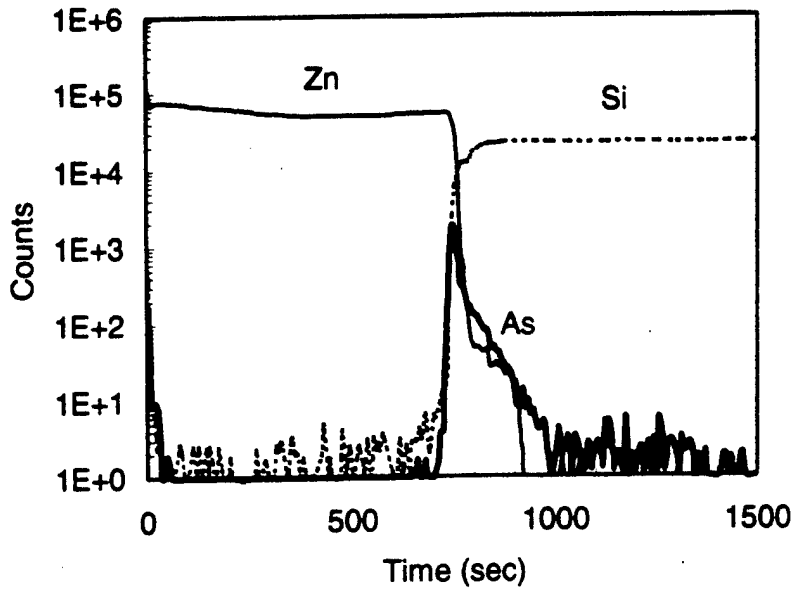

Figure 13 SIMS profile of a ZnS/As/Si(100) heterostructure

contamination was severe. Figure 13 is an example of a SIMS measurement for a sample grown in the single chamber arrangement. From this figure, we can see that there is diffusion of Si, Zn, and As at the interface. This diffusion of species is not desirable for laser applications since both the well layer and the barrier layer in a quantum well structure must be thinner than 100 Å. Clearly, this interface diffusion problem had to be solved if we were to use this material for inter-subband laser devices.

As described above we installed a new growth chamber and linked it to an existing Si growth chamber and a III-V reactor. Because of the extensive apparatus modifications, we were forced to recalibrate and tune all the growth conditions. This took several months to complete, however the growth steps for Si, ZnS, and As were totally separated and the cross contamination was sharply reduced. Several of these improvements were seen in various types of measurements, as reported below.

(b) New process to improve thin-layer growth

Because we were able to separate the growth processes with the new apparatus arrangement, we developed a new process to planarize the ZnS layers. This allowed growth of thinner ZnS-barrier

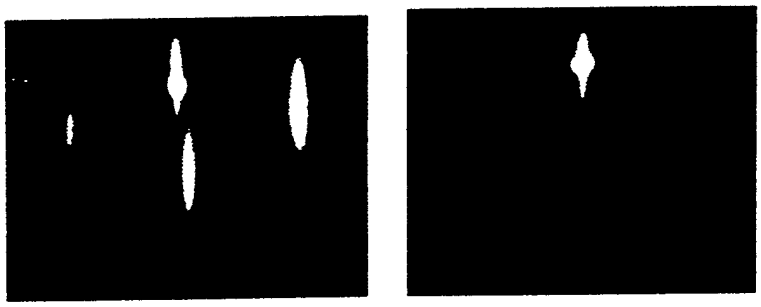

Figure 14 RHEED images of a 200 Å ZnS layer before (left) and after annealing (right). Annealing tended to merge the separate spots into a central streak.

layers. The new process also helped improve the surface of the ZnS barrier layers before Si growth. We also learned from the use of this new process how to deposit Si cap layers without passivating the ZnS surface. However, the growth of Si back on ZnS was not sufficiently well controlled to achieve thin layers of Si. We are presently working on ways to overcome this limitation as discussed later.

An important feature of the new growth procedure was an annealing step that involved ramping up the substrate temperature to 480 °C for several minutes after layer growth in the II-VI chamber where there was a residual ZnS background pressure. We found that this annealing technique would not work in other chambers where the background pressure came from species other than ZnS. Evidence of an *in situ* improvement was seen by a surface smoothing effect, as displayed by streakier RHEED patterns. In Figure 14, the RHEED pattern on the left was from an as-grown layer. The pattern on the right was from a layer after annealing. The elongated spots in the central streak were seen to lengthen and merge after annealing. This demonstrated that two-dimensional growth had been improved. Furthermore, it meant that thinner layers could be grown more reliably.

(c) Precise control of the thicknesses of both Si and ZnS epitaxial layers

With the improvements brought about by the apparatus modifications, we could control the growth rate much better and this allowed more control over the epitaxial layer thickness. Figure 15 shows examples of this thickness control in two cross-sectional TEM micrographs of samples grown in the new apparatus.

From Figure 15 one clearly sees that very thin ZnS layers could be grown on Si substrates and that the thickness of the ZnS layers could be finely controlled as well.

In addition to gaining control of the thickness, we were able to grow epitaxial layers more uniformly, with fluctuations of less than 5%. Before we installed the new growth chamber system, the thickness fluctuations were about 10%.

The improved apparatus also allowed successful growth of Si epitaxial layers on ZnS layers to form Si/ZnS/Si single-barrier structures as shown in Figure 16. From the TEM image in Figure 16, we see that the quality of the epitaxial Si cap layer was quite good. What then limited our ability to grow thin Si quantum wells was that we could not establish reliable growth conditions from one run to the next. We believe that the cause of this problem was that the flux from the Si e-beam source was shifting from one day to the next. After considerable effort, we finally managed to stabilize the

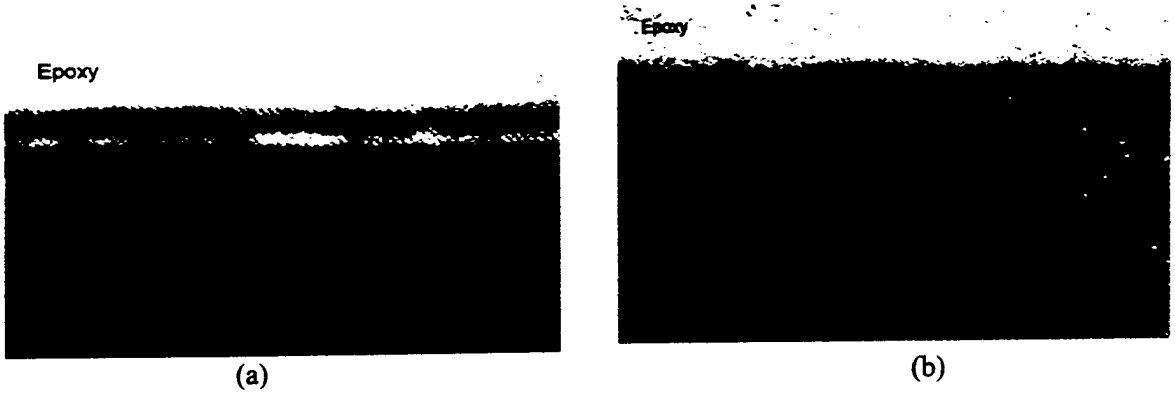

Figure 15 Two high resolution TEM images, the ZnS layers were designed to be 1.9 nm and 3.6 nm respectively in (a) and (b), the actual results in (a) and (b) are 1.7 nm and 3.4 nm which was close to the desired thicknesses.

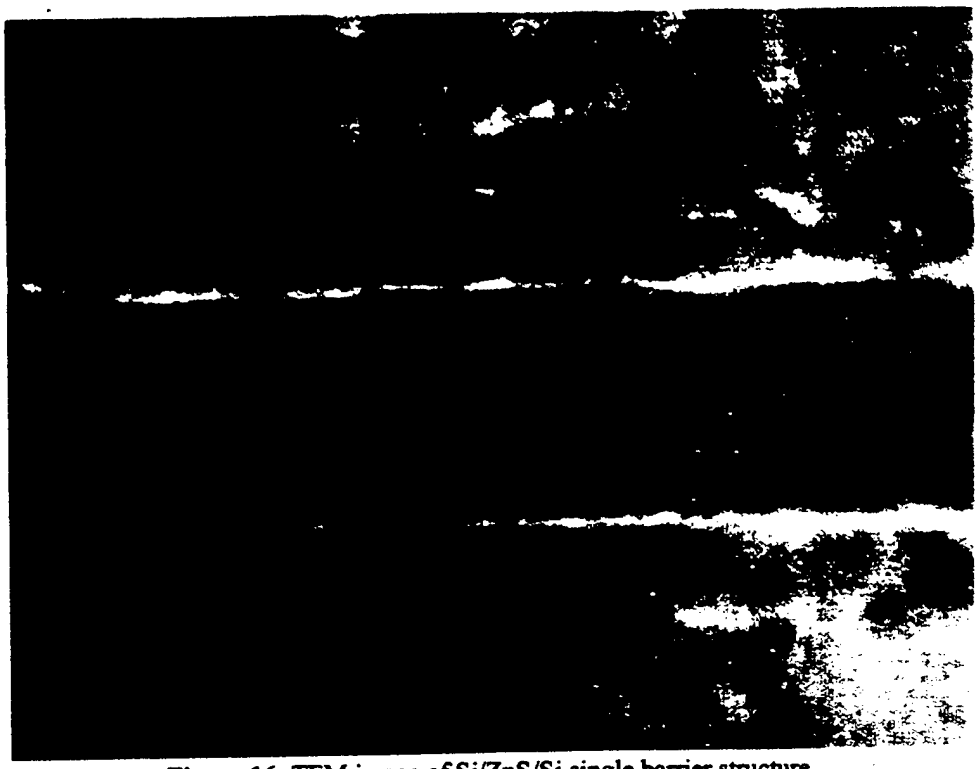

Figure 16 TEM image of Si/ZnS/Si single barrier structure.

e-beam source, but we have not yet had time to demonstrate that consistent growth can be achieved.

(d) Reduced interface charge density in ZnS and ZnS/Si interface

After installation of the new II-VI chamber and growth of several new ZnS/Si heterostructures, we fabricated several ZnS/Si metal-insulator-semiconductor (MIS) structures. Capacitance-voltage (C-V) measurements were done as one of several methods to check for improvements in terms of electrical properties. Figure 17 shows an example of such a measurement. From these types of high-frequency C-V measurements we were able to determine the fixed charge density, assuming that it is located at the ZnS/Si interface. In particular, the fixed charge density at the ZnS/Si interface was found to be only 3.3×10^{-7} C/cm^2 for structures grown in the new apparatus. By comparison to previous conditions, this result is smaller than the fixed charge density measured in ZnS/Si MIS structures (over 5×10^{-7} C/cm^2) grown by the earlier single chamber apparatus.

In addition, from the high-frequency C-V results, the interface state density was measured. This result is shown in Figure 18. It can be seen from Figure 18 that the interface state-density is low, in the mid 10^{11}cm^{-2}V^{-1} range. A low interface state-density is very important for producing light emitting diodes (LEDs) and laser diodes (LDs) since high interface state-density will dramatically decrease the emission efficiency of LEDs or LDs.

(e) Reduced mobile charge in ZnS

Not only is a low interface state-density and interface fixed charge density important, but the occurrence of mobile charge in the ZnS layer is also important. Its presence can strongly affect device quality. Using bi-directional voltage sweeps in high-frequency C-V measurements, we were able to investigate the behavior of the mobile charge density in our samples. For example, in Figure 19 we see that the hysteretic behavior of the voltage sweep was quite small. As is well known, pronounced hysteretic effects in C-V measurements are caused by mobile charges in the insulator

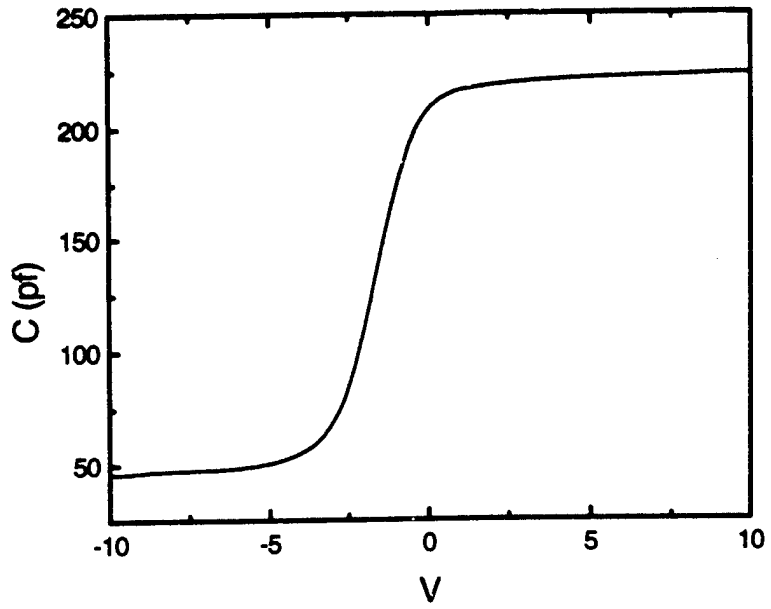

Figure 17 C-V measurement at one MHz frequency; thickness of ZnS layer is 100 nm.

layers of the samples. A negligible or small hysteresis implies a very small mobile charge. When compared to our old samples, these results showed that we have reduced the mobile charge density by at least an order of magnitude and that the new results are much more uniform from sample-to-sample.

In summary, from the high-frequency C-V measurements we found that the electrical properties of the ZnS/Si heterostructures were improved considerably due to the installation and modifications of the growth apparatus. Although, some interface states, as well as fixed and mobile charges remain, the improvements have been significant. Another important parameter that demonstrated

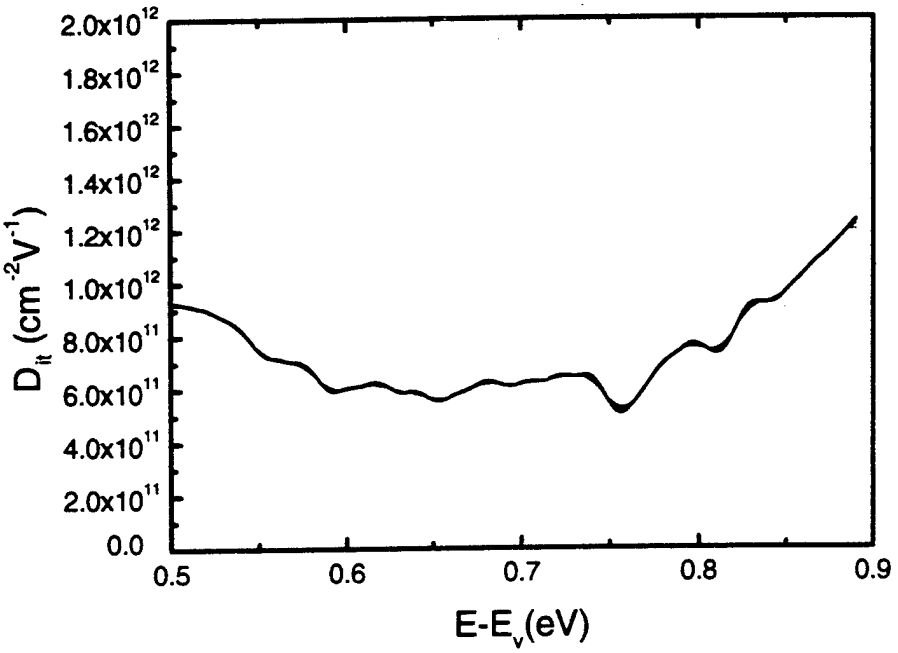

Figure 18 ZnS/Si interface state density.

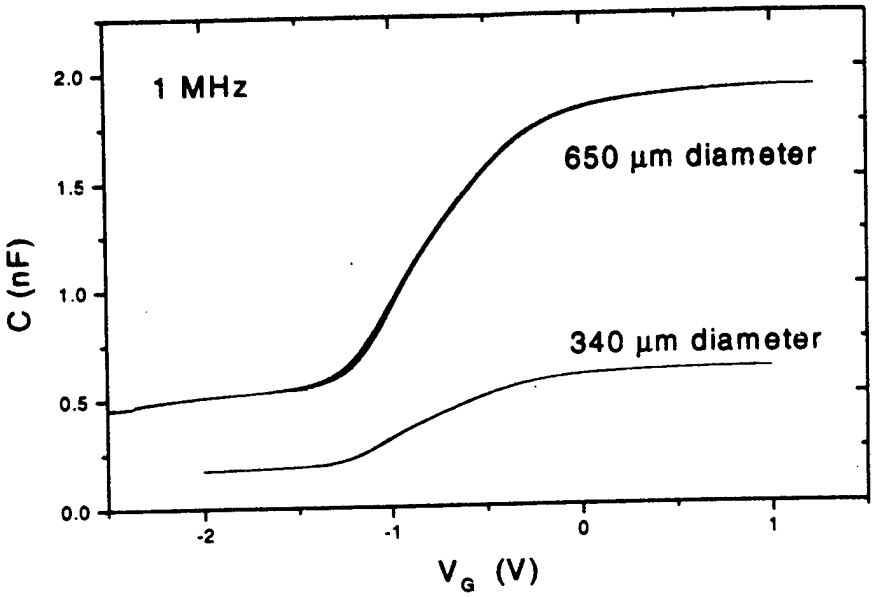

Figure 19 Bi-directional-voltage sweeps of C-V measurements at high-frequency.

the uniformity of the material across the wafer is the number of operational devices per slice. For example, when we made 10 MIS devices using materials grown by the new growth system, we found that 90 % or better of them were good and that the electrical properties were very similar. By comparison, when we made 10 MIS devices using materials grown by the earlier one-chamber growth system, we found only about 10 % of these devices were good. Thus, the improved device yield was another important indication that improvement resulted from the apparatus modifications.

7. Development of New Materials

After reviewing our experience with growing ZnS/Si heterojunction structures, we concluded that this material is potentially useful for laser devices. However, we also appreciated the limitations this particular material system presented in terms of thermal stability at high growth temperatures needed in Si deposition on ZnS and of zinc sulfide's low stacking fault energy. With this knowledge in hand we reviewed other wide bandgap materials with the requirement that they be good candidates for growing Si-based heterostructures. An additional criterion was that they form quantum well structures with band-offsets suitable for laser applications. A promising candidate group was the beryllium chalcogenide II-VI-compound materials, such as BeTe, BeSe, BeS, and the related ternary compound materials that could be formed. The lattice constants and corresponding bandgap values are shown in Figure 20 for several of these compounds. As can be seen from Figure 20 the lattice of $BeTe_xSe_{1-x}$ can be varied from 5.2 Å to 5.6 Å by adjusting the composition x. This suggests that a composition of x= 0.55 should result in $BeTe_{0.55}Se_{0.45}$ being lattice matched closely with Si. The bandgap of $BeTe_{0.55}Se_{0.45}$ would then be about 3.2 eV, which is high enough to make a good wide bandgap candidate for a Si-based inter-subband laser device. The band offset is yet to be determined.

Recently we investigated the growth of BeTe on Si [Zhou, Jiang, and Kirk, J. Crystal Growth, **175/176**, 624 (1997)]. Figure 21 shows a TEM micrograph of a BeTe sample grown on Si. We see that even though the lattice constants of BeTe and Si are mismatched by 4%, the TEM picture in Figure 21 indicates that a good epitaxial BeTe layer formed on the Si substrate. Although these data are preliminary in nature, the crystal quality of the BeTe layer appeared to be much better than the results we obtained from some of the ZnS growth on Si.

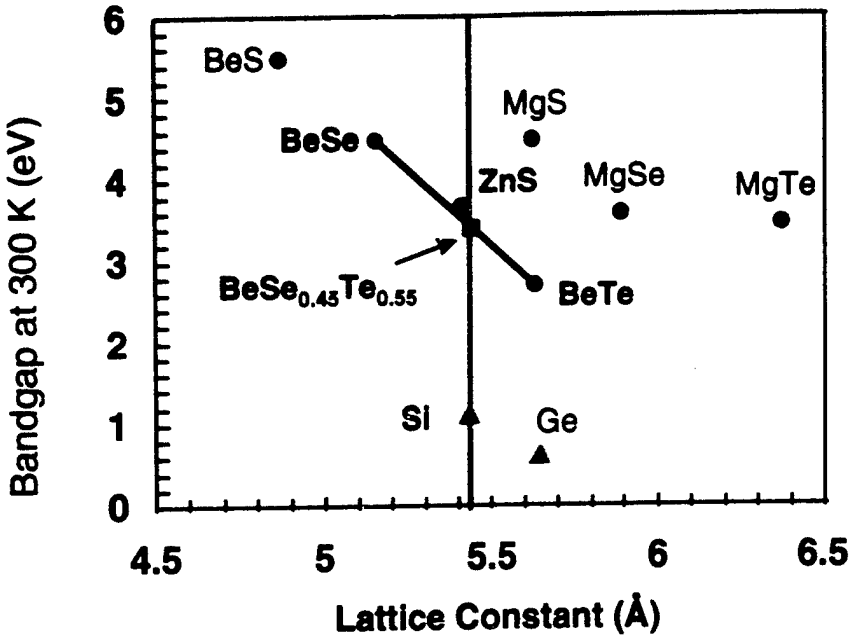

Figure 20 Lattice constant and band gap of Be based II-VI compounds.

Besides the TEM result, we also made an I-V measurement on a BeTe/Si MIS structure. This result is shown in Figure 22. Here we see that the BeTe layer acted like an insulator, due to its wide bandgap property. The leakage current was less than 5×10^{-7} A/cm^2 at a bias voltage of 5 V, which is an encouraging sign.

It is clear from the TEM and I-V results that the Be-chalcogenide compounds are promising candidates for Si-based quantum well structures, and that they might be used effectively in fabricating laser and optical waveguide devices. Because of this favorable situation, one of our next steps will be to try to grow $BeTe_{0.55}Se_{0.45}$ on Si and thus take steps to make a lattice-matched quantum well structure on Si. Along with the growth work, we will continue to characterize these

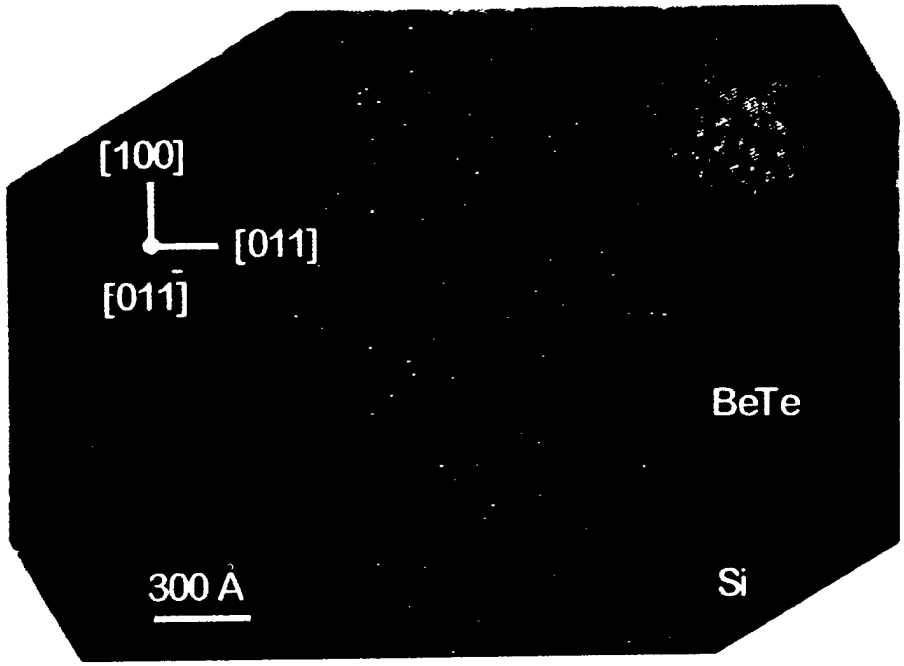

Figure 21 Cross-section TEM micrograph of a BeTe/Si sample.

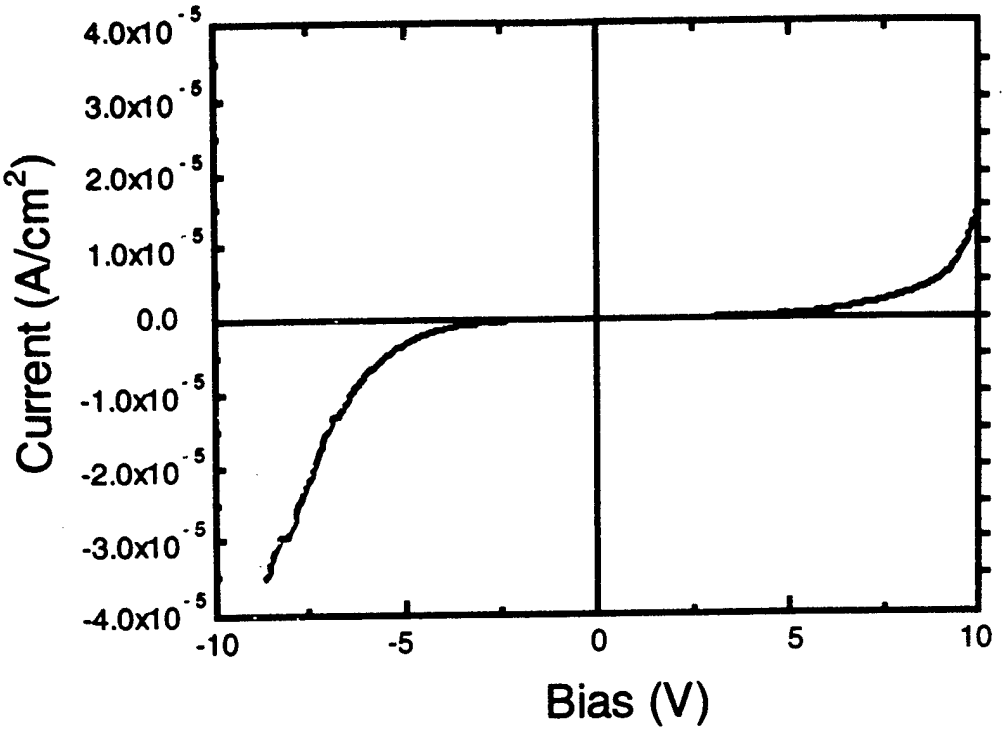

Figure 22 Dependence of current density on bias voltage for a MIS BeTe/Si heterojunction.

new materials with electrical and optical measurements so that we can understand the critical steps needed to form an inter-subband laser structure.

Very recently we succeeded in growing BeSe and BeSeTe (of unknown composition) on Si. Both of these materials are single crystals. Using a model 1280 *n&k* analyzer from *n&k* Technology, we determined some important optical parameters for these samples, *viz.* the index of refraction $n(\lambda)$, extinction coefficient $k(\lambda)$, and film thickness d. These results are shown in Figure 23. From these measurement one can determine the bandgap values of the films. In the case of the BeSe and BeSeTe films, we obtained 4.5 eV and 4.2 eV, respectively. These results were similar to the values shown in Figure 20.

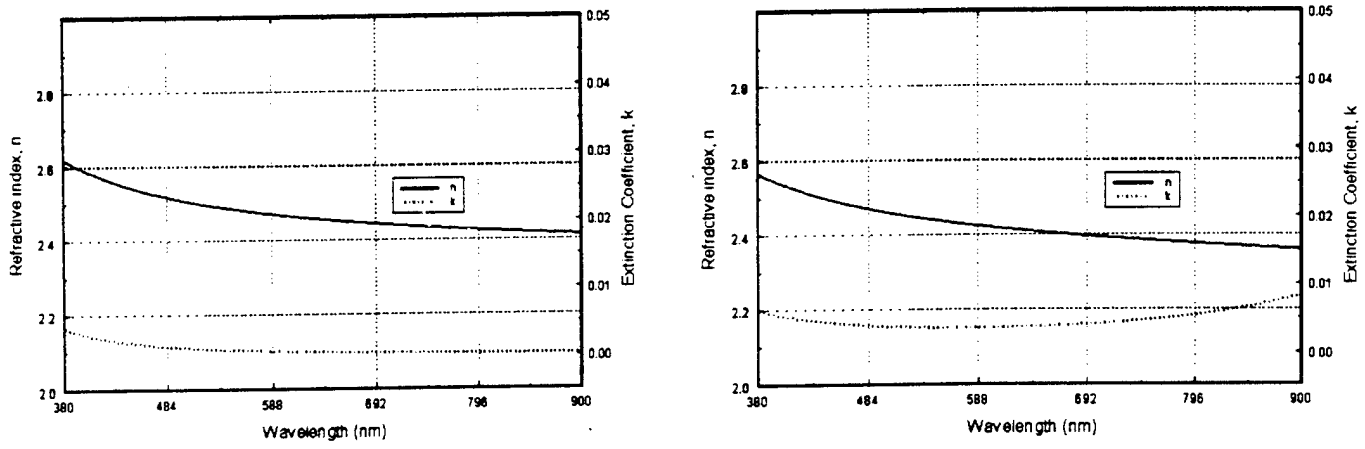

(a) (b)

Figure 23 Optical characterization using n&k analyzer, (a) is BeSe, and (b) BeSeTe.

Personnel Supported in Part by this Program

Professional personnel:

Dr. Wiley P. Kirk, Professor and Director, PI
Dr. X. Joe Zhou, Research Scientist and Associate Director
Dr. Abdullah Cavus, Research Scientist and Associate Director
Mr. Robert T. Bate, Senior Research Scientist
Mr. Eduardo Maldonado, Research Instrumentation Specialist
Mr. Robert Klima, Research Instrument Specialist

Post doctoral:

Dr. Shan Jiang, Research Associate

Graduate students:

Mr. Tiecheng Zhou
Mr. Hong Jiang

Undergraduate students:

Mr. Andrew Wolven

Publications

1. *Epitaxial growth of ZnS on bare and arsenic-passivated vicinal Si(100) surfaces*, Xiaochuan Zhou, Shan Jiang, and Wiley P. Kirk, J. Appl. Phys. **82** (4), 2251-2262 (1997).
2. *Band offset study of ZnS/Si heterojunction*, S. Jiang, X. Zhou, T. Zhou, K. P. Clark, G. Spencer, R. T. Bate, W. P. Kirk, R. M. Steinhoff, and B. Brar, Proc. IEEE 24th Intl. Symp. On Compound Semiconductors (San Diego, CA, 1997) pp 167-170.
3. *Electrical properties of ZnS layer grown on Si(100)*, S. Jiang, X. Zhou, T. Zhou, and W. P. Kirk, Phys. Rev. B (in preparation).
4. *Molecular beam epitaxy of BeTe on vicinal Si(100) surfaces*, X. Zhou, S. Jiang, and W. P. Kirk, J. Crystal Growth **175/176,** 624-631 (1998).

Interactions and Transitions

We collaborated with Dr. Richard A. Soref at USAF Rome Laboratory on the development of silicon-based multi-quantum well structures for intersubband lasers. We prepared samples for his group to run optical characterization experiments using PL and FTIR.

Part of this work was supported and reported under AFOSR F49620-96-C-0006 as a subcontract from Raytheon Systems. In this collaboration we worked with Dr. Alan Seabaugh at Raytheon Systems on Quantum MOS Technology in which the ZnS/Si system offered the possibility of building room temperature resonant tunneling devices for nanoelectronics applications. See details below.

Exploration of new technology: silicon on lattice-matched insulators, using BeSeTe in advanced CMOS as gate and interlevel insulating layers. The NanoFAB Center under separate contract with DARPA Advanced Microelectronic program is carrying out this work.

Other DoD interactions

Research Result Transferred:

Multiple materials systems were investigated and used to fabricate heterojunctions such Si/SiO_2 and Si/ZnS, which in turn were used to determine the best approach for resonant tunneling integration. Also, materials characterization measurements, and elementary electrical property measurements were supplied.

Recipient of Technology Transfer:

Dr. Alan Seabaugh
Raytheon Systems Company
Under AFOSR contract: F49620-96-C-0006

Application: (how recipient is using research results)

The program goal of Raytheon Systems was to demonstrate CMOS-compatible resonant tunneling diodes (RTDs) for integration with CMOS (complementary metal oxide semiconductor) technology and to design circuits that exploit the speed-power advantage of integrated RTD and CMOS devices. This program was in response to DARPA's requirement for silicon-based nanoelectronics for ultra-dense, high-speed computing and electronic components.

Participation in conferences:

1. **Using Be-VI as a Means of Reducing Stacking Faults in Wide-bandgap II-VI Semiconductor Epitaxial Materials**, X. Zhou, contributed talk, 9th International Conference on MBE, San Diego, CA [Aug 5-9, 1996].
2. **Silicon-Based QMOS**, W. P. Kirk, briefing, Texas Instruments annual QMOS Workshop, Dallas, TX [April 22-23, 1997].
3. **New II-VI Wide Bandgap Materials for Visible Light Emitters**, A. Cavus, invited talk, Workshop on Compound Semiconductor Materials and Devices, San Antonio, TX [Feb 16-18, 1997].
4. **Molecular Beam Epitaxy of BeTe on Vicinal Si(100) Surface**, W. P. Kirk, invited talk, Workshop on Compound Semiconductor Materials and Devices, San Antonio, TX [Feb 16-18, 1997].
5. **New II-VI Wide Bandgap Materials for Visible Light Emitters**, A. Cavus, invited talk, Texas Instruments seminar, Dallas, TX [March 5, 1997].
6. **Development of Wide Bandgap ZnS/Si and BeTe/Si Heterostructures for Silicon-Based Electronic Devices,** W. P. Kirk, poster presentation, Silicon Heterostructures: From Physics to Devices Conference at Castelvecchio Pascoli, Italy [September 15-19, 1997]
7. **Silicon-Based QMOS**, W. P. Kirk, briefing, Raytheon-TI Systems annual QMOS Workshop, Dallas, TX [April 1-3, 1998].
8. **BeTe/Si Heterostructures for MIS and Quantum Device Applications**, W. P. Kirk, contributed talk, 1998 IEEE Si Nanoelectronics Workshop, Honolulu, HI [June 7-8, 1998].

New Discoveries, Inventions and/or Patent Disclosures

None

Honors and Awards

Recipient:

Wiley P. Kirk

Robert T. Bate

Institution:

Texas Engineering Experiment Station, Texas A&M University System

Type of Award:

Equipment grant

Heterostructure Growth System for Silicon-Based Nanoelectronics

DURIP Proposal Topic #13, 1996

Reason for Award:

Using this award we added a molecular beam epitaxy growth chamber to two existing MBE machines to make a multi-growth-chamber MBE system. The multi-growth-chamber system is used in materials growth for the development of silicon-based electronic and electroptic applications (topic 13 of the DURIP announcement). The goal of the research was to develop an appropriate material system that is compatible with silicon substrates and silicon processes.